Combustion and Flame 161 (2014) 2203–2208

Contents lists available at ScienceDirect

Combustion and Flame

journal homepage: www.elsevier.com/locate/combustflame

Assembly and reactive properties of Al/CuO based nanothermite microparticles

Haiyang Wang [1], Guoqiang Jian, Garth C. Egan, Michael R. Zachariah *

Department of Chemical and Biomolecular Engineering, University of Maryland, College Park, MD 20742, United States
Department of Chemistry and Biochemistry, University of Maryland, College Park, MD 20742, United States

ARTICLE INFO

Article history:
Received 4 September 2013
Received in revised form 18 November 2013
Accepted 7 February 2014
Available online 22 March 2014

Keywords:
Nanoenergetics
Thermite
Micron particles
Heterogeneous combustion

ABSTRACT

It is generally agreed that a key parameter to high reactivity in nanothermites is intimate interfacial contact between fuel and oxidizer. Various approaches have been employed to combine fuel and oxidizer together in close proximity, including sputter deposition [1], and arrested milling methods [2]. In this paper, we demonstrate an electrospray route to assemble Al and CuO nanoparticles into micron composites with a small percentage of energetic binder, which shows higher reactivity than nanothermite made by conventional physical mixing. The electrospray approach offers the ability to generate microscale particles with a narrow size distribution, which incorporates an internal surface area roughly equivalent to the specific surface area of a nanoparticle. The size of the micron scale composites could be easily tuned by changing the nitrocellulose content which is used as the binder. The composites were burned in a confined pressure cell, and on a thin rapidly heated wire to observe burning behavior. The sample of 5 wt.% nitrocellulose showed the best response relative to the physical mixing case, with a 3× higher pressure and pressurization rate. The ignition characteristics for these micron particles are essentially equivalent to the nanothermite despite their significantly larger physical size. It appears that electrospray assembly process offers to potential advantages. 1. Enhanced mixing between fuel and oxidizer; 2. Internal gas release from nitrocellulose that separates the particles rapidly to prevent sintering. The later point was shown by comparing the product particle size distribution after combustion.

Published by Elsevier Inc. on behalf of The Combustion Institute.

1. Introduction

Nanothermites, are a class of energetic material containing both fuel (aluminum) and oxidizer (CuO, Fe_2O_3, MoO_3, Bi_2O_3, etc.) which undergo a very rapid redox reaction [3]. They have found applications as gas generators [4,5], in nano-scale welding [6,7], micropropulsion [8,9], ammunition primers [10] and electric igniters [11,12], as well as energetic additives in explosives and propellants [10,13,14].

Decreasing the size of conventional thermite to the nanoscale greatly increases the interfacial contact, and reduces the diffusion distance between fuel and oxidizer, thus resulting in a significantly enhanced reactivity [6,15–18]. Moreover, it has been observed that both ignition delay and ignition temperature are also decreased when micro-sized particles are replaced by nanoparticles [19].

The easiest and most common approach to create an intimate mixture between fuel and oxidizer is simple physical mixing with nanoparticles. More sophisticated assembly methods include, sputtering [1,20–22], arrested reactive milling (ARM) [2,23,24], electrostatic directed assembly [25], and sol–gel synthesis [26,27]. In recent years, self-assembly approaches have been employed to precisely engineer three-dimensional structural nanothermites [28]. Polymers and ligands have also been employed as linkers to assemble fuel and oxidizer nanoparticles. Subramanium et al. reported self-assembled fuel nanoparticles around an oxidizer matrix using poly(4)-vinyl pyridine (P4VP) [29,30]. Malchi et al. employed charged ligands ($COOH(CH_2)_{10}NMe_3^+Cl^-$, $SH(CH_2)_{10}COO^-NMe_4^+$, etc.) on n-Al and n-CuO to create ~1–5 μm microspheres via electrostatic self-assembly [31]. In our previous study, we also found a significant increase in reactivity when oppositely charged fuel and oxidizer nanoparticles were assembled [25]. More recently, Rossi et al. demonstrated a DNA-directed assembly procedure to produce highly energetic nanocomposites by assembling Al and CuO nanoparticles into microparticles [32]. All these studies show the same general result, that intimate interfacial contact results in high reactivity.

In this paper, we demonstrate the preparation of Al/CuO micron-sized nanothermites by electrospraying Al and CuO

* Corresponding author.
E-mail address: mrz@umd.edu (M.R. Zachariah).
[1] Address: Nanjing University of Science and Technology, Nanjing 210094, China.

http://dx.doi.org/10.1016/j.combustflame.2014.02.003
0010-2180/Published by Elsevier Inc. on behalf of The Combustion Institute.

nanoparticles suspensions containing a dilute nitrocellulose solution. This work builds on some of our prior work in which electrospinning (a close cousin to electrospray) was first used to create thermite based nanofiber mats [14], and more recently an electrospray approach was employed to produce nanoaluminum microspheres [33]. By changing either particle loading or polymer concentration, we were able to tune the size and composition of the aluminum microparticles, consequently the burning performance of the Al/NC composites was easily tuned.

In this work, we extend the approach to create nanothemite composite microparticles of Al/CuO, and evaluate the reactivity in comparison to the corresponding physically mixed case. Electrospray offers several advantages, including the ability to change the final particle size of the composite, a narrow final particle size distribution, ambient temperature/pressure operation to enable the incorporation of polymer binders, and or thermally labile molecular additives, and the ability to be scaled-up [34,35]. First we find enhanced burning properties of this type of thermite composite which may be related to both better mixing between fuel and oxidizer and a decreased amount of sintering observed in the product particles. An important benefit appears to be the ability to generate microscale particles, which incorporates an internal surface area roughly equivalent to the specific surface area of a nanoparticle. This latter situation is a potential advantage in the formation of polymer composites with high mass loadings of nanoparticles, which has previously been difficult to achieve due to the high viscous resistance that nanoparticles induce in a polymer mix.

2. Experimental

2.1. Materials

Copper oxide (CuO, ~50 nm) nanoparticles were purchased from Sigma–Aldrich Corporation, and aluminum (Al, ~50 nm) nanoparticles were purchased from Argonide Corporation, and used as received. Collodion solutions (4–8 wt.% in ethanol/diethyl ether) were purchased from Fluka Corp and diethyl ether (99.8%)/Ethanol (99.8%) mixture (volume ratio: 1:3) was used to dilute the collodion solution. Al nanoparticles were determined to contain ~70 wt.% active aluminum by thermogravity analysis (TGA) [36].

2.2. Precursor preparation procedure

CuO nanoparticles were firstly ultrasonicated for 1 h in ethanol, to which nano aluminum was gently added, followed by the diluted collodion solution. In a typical experiment, 180 mg of Al nanoparticles, and 540 mg CuO nanoparticles were dispersed in 0.8 ml ether, and 2.4 ml ethanol, together with 1.4 ml of the collodion solution (10 wt.% NC). The as prepared suspension was sonicated for another 1 h, and magnetically stirred for 24 h.

2.3. Electrospray

A syringe pump was employed to feed the precursor at a fixed rate of 4.5 mL/h, through a 0.43 mm inner diameter stainless steel nozzle. To form a stable Taylor cone (see Fig. 1) suitable for electrospray, (+) 10 kV and (−) 9 kV were applied to the nozzle and substrate, respectively, and the resulting droplets were given sufficient flight time (distance to substrate ~10 cm) for solvent evaporation to form solid particles deposition on the conducting substrate.

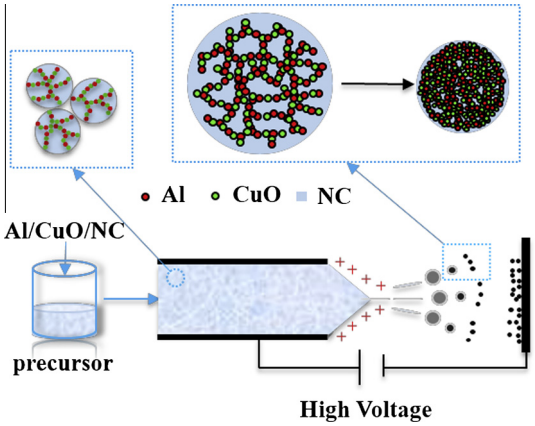

Fig. 1. Electrospray formation of nanostructured microparticles.

2.4. Conventional physical mixing

For characterization of the physically mixed samples, the precursor was placed in a fume hood for 24 h to completely dry, and then subsequently broken into a loose powder.

2.5. Combustion cell characterization

Combustion performance was evaluated with a confined combustion cell of constant volume (~13 cm^3), which can simultaneously measure the pressure rise and optical emission. In this work, 25.0 mg of sample was place in the combustion cell, and ignited by joule heating with a nichrome coil. The pressurization rate (dP/dt) is defined as the initial slope of the pressure rise, and the FWHM burn time is defined as the full-width half-maximum of the optical emission curve. Each sample was evaluated in triplicate and the average values reported. The details of this system can be found in our previous works [18,37].

2.6. T-jump wire ignition

The details of the T-jump wire ignition experiments, and the operational setting can be found in our previous works [18,36,38]. Typically, a platinum filament of ~11 mm long, 76 μm diameter coated with nanothermite sample (~4 mm long) was ramped to ~1600 K in 3 ms, at a heating rate of ~4×10^5 K s^{-1} to ignite the sample. From the temporal current and voltage, the calculated resistivity can be converted to temperature to determine the ignition temperature. High-speed digital video imaging of the combustion process was recorded with a Vision Research Phantom® v9.1 digital camera, at a frame rate of 67,000 frames per second and a resolution of 256 × 256.

3. Results and discussion

3.1. Electrospray formation of Al/CuO/NC microparticles

As shown in Fig. 1, the electrospray process is a one-step process, in which fuel and oxidizer nanoparticles within micrometer droplets aggregate during solvent evaporation, to generate a highly porous microparticle. The nominal advantage of electrospray over other spray methods is that electrospray generates a much narrower droplets size distribution with smaller droplets.

A scanning electron microscopy (SEM) image for a typical Al/CuO sample (10 wt.% NC) is shown in Fig. 2. Figure 2a shows the as deposited particles on the sample collector substrate, forming a 100 μm thick layer (Fig. 2a-1), with nominal diameters of

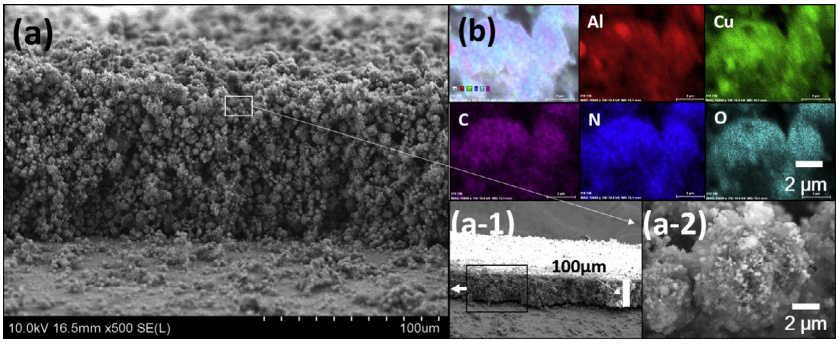

Fig. 2. SEM images (a), elemental mapping (b) of Al/CuO microparticles produced by a typical electrospray process. (NC: 10 wt.%).

~5 μm (Fig. 2a-2). Elemental mapping of the individual microparticles, and X-ray energy disperse spectrum (EDS) (Fig. 2b) show that Al and CuO are in a well mixed state and that the NC is distributed homogenously within the microparticles. The purpose of adding NC are twofold.

First by changing the NC content in the precursor solution, products with different morphologies and size distributions were prepared, and in this function NC acts as a binder. The NC also serves the function of a gas generator within the particle which as we shall show impart some interesting combustion properties. As Fig. 3a shows, the SEM image of the sample produced from precursor solutions containing 1 wt.% NC show no obvious spherical microparticles, and are relatively small compared to the microparticles shown in Fig. 2 (10 wt.%). It appears that NC acts as a binder to hold the jammed aggregates into a structure that upon deposition retains their physical shape to prevent disintegration. Increasing the NC content to 3 wt.%, we observe microparticles (Fig. 3b), but with a very wide size distribution that make discerning individual particles difficult.

The threshold to create distinct microparticles appears to be ~5 wt.%, where spherical microparticles are easily discernible and particle size histograms can be generated. Increasing NC content from 5 wt.% to 15 wt.%, was found to increase the average microparticle size from ~3 μm to ~6 μm. Since the nanoparticle loadings were not changed in the precursor solution, the increase of particle size implies that larger droplets are produced during electrospray at higher concentrations of NC, presumably due to an increase in viscosity of the precursor solution [39].

3.2. Combustion cell results and the role of mixing in combustion performance

The combustion performance of thermite samples was evaluated by igniting 25.0 mg of thermite sample in a combustion cell, instrumented with a fast response pressure transducer and an optical emission sensor. The results for maximum pressure, pressurization rate and burning time as a function of NC content are presented in Fig. 4. Results for conventional physical mixing are also plotted for comparison.

As shown in Fig. 4a and b, both maximum pressure and pressurization rate decrease with increasing NC content for Al/CuO nanothermite sample prepared with a conventional physical mixing method. In contrast, for the electrosprayed particles, we find that both maximum pressure and pressurization rate show a significant increase with increasing NC content up to 5 wt.%, where the microparticles have maximum pressures and pressurization rates of ~3.4 and ~8.8 times larger than the corresponding physically mixed thermite. Above a concentration of 5 wt.%, the electrosprayed microparticles show a rapid decrease on both pressure and pressurization rate. Burning times shown in Fig. 4c, indicate that NC content has little impact for concentrations below ~6 wt.%, but at higher concentrations a significant increase in burning time is observed particularly for the physically mixed sample, which appears to be very sensitive to NC content. Cheetah thermochemical calculation for 25.0 mg Al/CuO/NC in a 13 ml closed cell, shows a monotonic increase in the product pressure with NC content, and thus does not capture the features observed

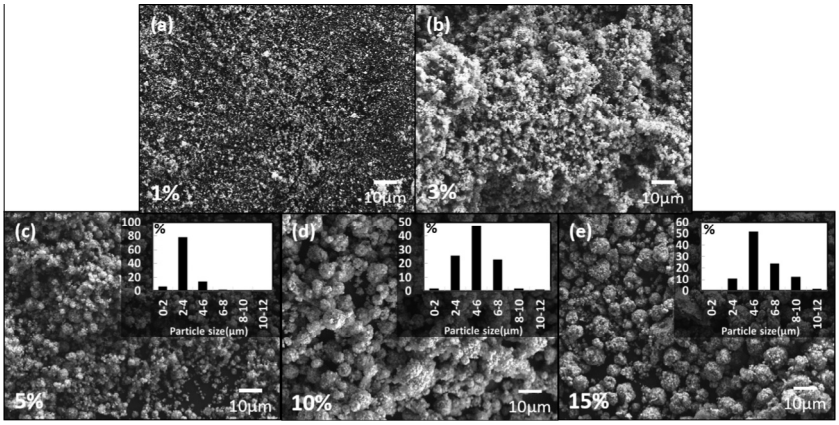

Fig. 3. SEM images of nanothermite made by electrospray with NC content of 1 wt.% (a), 3 wt.% (b), 5 wt.% (c), 10 wt.% (d) and 15 wt.% (e). Inserts are histograms of the size distribution.

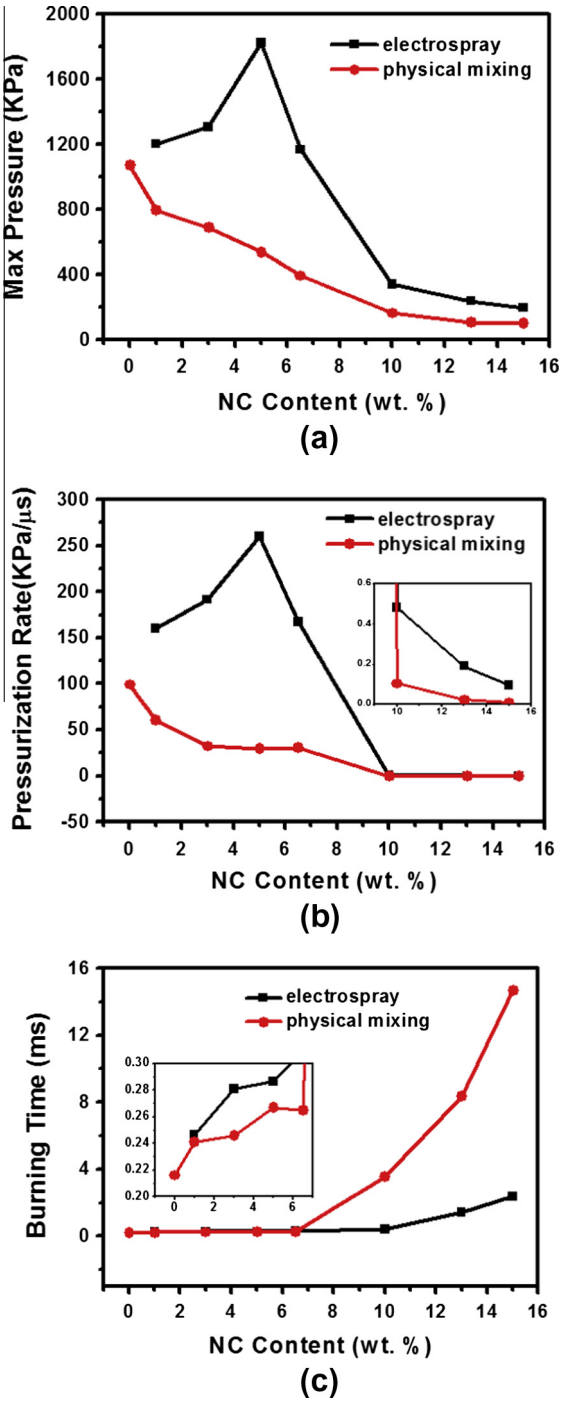

Fig. 4. Maximum pressure (a), pressurization rate (b) and burning time (c) of the nanothermite samples prepared by electrospray and physical mixing as a function of NC content.

experimentally. This is not surprising since the differences in reactivity between the physically mixed and microparticles are only due to the nature of the nanostructuring since they are chemically identical.

It is widely accepted that the interfacial contact between the fuel and oxidizer plays an important role in the combustion performance of composite energetic materials e.g. nanothermites. The enhanced combustion performance of the electrosprayed microparticles relative to the physically mixed material are suggestive of superior intermixing of the two components. Figure 5 shows SEM images and the elemental maps of samples made by electrospray and physical mixing with 5 wt.% NC content. Clearly, different mixing and dispersion can be observed in the two samples, as schematically shown in Fig. 5a and d. For thermite samples prepared by electrospray shown in Fig. 5b and c, fuel and oxidizer nanoparticles were well dispersed in the microparticles, with intimate contact between fuel (Al) and oxidizer (CuO) as confirmed by elemental mapping. In contrast, the thermite sample prepared by physical mixing in Fig. 5e and f shows clear segregation.

Since NC exists in the precursor solutions of both thermite samples, it is reasonable to conclude that the electrospray process contributes to better dispersion of fuel and oxidizer nanoparticles resulting from the strong capillary forces that will collapse all the particles together during the very rapid solvent evaporation process.

3.3. T-Jump wire ignition results and the role of gas release in combustion performance

T-jump wire ignition studies shown in Fig. 6 indicate that the electrosprayed sample shows a more homogenous fireball (related video is in supporting material). In contrast, the physical mixing nanothermite, especially the no-NC case (not shown), shows a more heterogeneous structure, with very large particle burning, consistent with significant sintering of the nanomaterial during combustion [40,41]. The ignition of the electrospray sample occurs ~0.15 ms earlier than the physical mixed case, which corresponds to ignition temperatures of 930 K and 1000 K, respectively. This implies that the ignition characteristics for these super micron particles are essentially equivalent to the nanomaterials despite their significantly larger physical size.

The images presented in Fig. 6 along with the enhanced combustion performance shown in Fig. 4 suggest that something beyond better mixing is also in play. In particular does the creation of a microparticle incorporating a gas generator delay the onset of sintering thereby preserving the nanostructure longer during the combustion event? To assess this possibility solid products of combustion were collected by placing a SEM substrate 2.0 mm from the T-jump wire. Figure 7 shows images from product samples for the "physically mixed" and the "electrosprayed material". As panels (a) and (b) show the electrosprayed reaction products have a much smaller particle size distribution than the corresponding physically mixed case. Higher magnification SEM image shows that the product particles in the physically mixed cases are several microns (1–10 μm) in size, while those from the electrospray reaction are mainly submicron (0.2–1.0 μm). This is also visible in the combustion images in Fig. 6 which show larger particles burning in the physically mixed case, relatively to the fine homogenous fire ball in the electrosprayed case.

NC functions beyond its role as a binder, to also serve as a gas generator. This latter point results in less sintering as evidenced by the more homogenous burning and the smaller product particles observed in Figs. 6 and 7. The fact that increased NC content in the physically mixed sample degrades performance while increasing it for the microparticle is intriguing. While we do not have a definitive understanding of the burning mechanism it is reasonable to speculate. At low NC content performance is increased, possibly due to the presence of a ready source of low temperature energetic, generating gas so as to prevent sintering. At higher loading, performance degrades because energy content is degrading, and possibly that we have reached a limit where too much gas generation only serves to dissipate the reactant from each other resulting in reaction quenching.

This latter explanation is consistent with our observation and explanation that localization of the heat release explains the superior reactivity of gelled Al microspheres in our previous work [33].

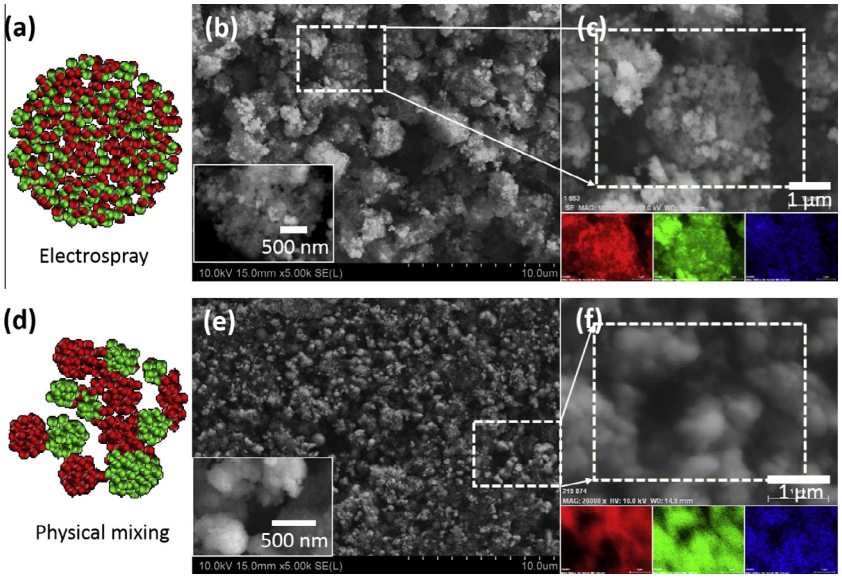

Fig. 5. SEM images and elemental mapping of the nanothermite made by electrospray (a, b and c) and physical mixing (d, e and f), 5 wt.% NC. Note: Aluminum (red); Copper oxide (green); Nitrogen (blue). (For interpretation of the references to color in this figure legend, the reader is referred to the web version of this article.).

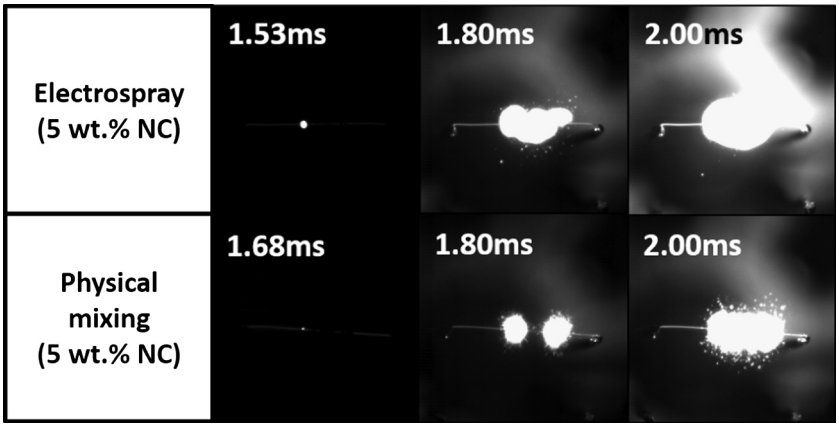

Fig. 6. High speed imaging of nanothermite (NC, 5 wt.%) burning on hot wire. Heating pulse: ~3 ms, heating rate: $\sim 5 * 10^5$ K/s.

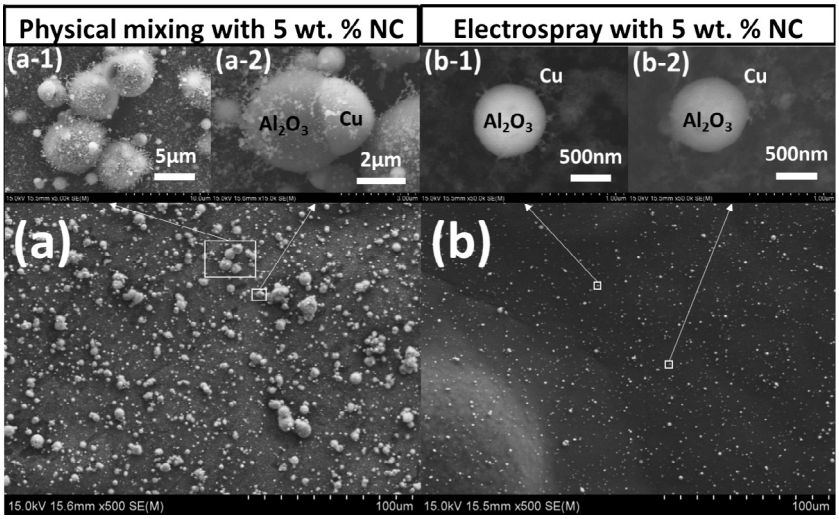

Fig. 7. Burned products collected from wire combustion experiments of physical mixed sample (a) and electrosprayed sample (b). Fig. 8a-1, 2 and Fig. 8b-1, 2 are SEM images with higher magnification. Note: The materials in Fig. 7a-1-2, and b-1–2 are confirmed by X-ray energy disperse spectroscopy. The results show that the products of combustion from the microparticles are significantly smaller indicating diminished sintering.

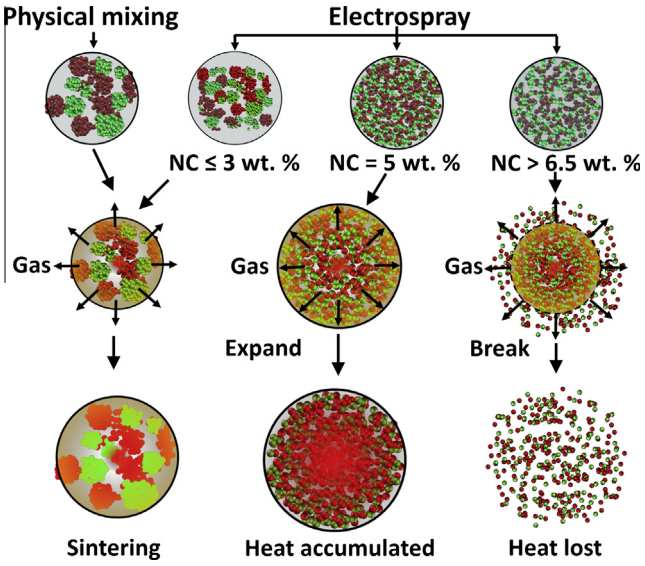

Fig. 8. Possible mechanisms of the burning of nanothermite made from physical mixing and electrospray. Note: Aluminum (red); Copper oxide (green); Nitrocellulose (light blue). (For interpretation of the references to color in this figure legend, the reader is referred to the web version of this article.).

The porous microparticles could accumulate the heat within the microstructure while promoting the mass transport at the same time. Instead of isolated or aggregated Al and CuO nanoparticles undergoing redox reaction with high heat loss to the surrounding, the microparticle may serve to accumulate some of the heat of reaction leading to a self-accelerating behavior. At some point adding additional NC (>6.5 wt.%,) apparently offers diminishing returns, by overpressuring the structural integrity of the microparticle (Fig. 8) and leading to its disintegration into smaller structures. At this point both pressure and pressurization rate drops sharply from the peak value to less than 400 kPa and 0.5 kPa/μs, respectively (from 5 wt.% to 10 wt.%). In fact, this also increases the burning time of the nanothermite microparticles, as shown in Fig. 4c.

4. Conclusion

In summary, we demonstrate electrospraying as a facile way to fabricate nanothermite microparticles with well mixed components. Nitrocellulose acts as a binder but also contributes to a lower ignition temperature of the thermite. The ignition characteristics for these super micron particles are essentially equivalent to the nanomaterials despite their significantly larger physical size. These materials also show pressure and pressurization rates that outperform physically mixed nanothermites. The key feature of the material is the creation of microparticles with specific surface area equivalent to individual nanoparticles. In this study, the electrospray process offers to potential advantages. 1. Enhanced mixing between fuel and oxidizer; 2. Internal gas pressure release that separates the particles rapidly to prevent sintering.

Acknowledgments

This work was supported by the Defense Threat Reduction Agency and the Army Research Office. We acknowledge the support of the Maryland Nanocenter and its NispLab. The NispLab is supported in part by the NSF as a MRSEC Shared Experimental Facility. Haiyang Wang is grateful for the financial support from China Scholarship Council.

Appendix A. Supplementary material

Supplementary data associated with this article can be found, in the online version, at http://dx.doi.org/10.1016/j.combustflame.2014.02.003.

References

[1] K.J. Blobaum, M.E. Reiss, J.M. Plitzko, T.P. Weihs, J. Appl. Phys. 94 (2003) 2915–2922.
[2] M. Schoenitz, T.S. Ward, E.L. Dreizin, Proc. Combust. Inst. 30 (2005) 2071–2078.
[3] D.G. Piercey, T.M. Klapötke, Cent. Eur. J. Energetic Mater. 7 (2010) 115–129.
[4] K.S. Martirosyan, J. Mater. Chem. 21 (2011) 9400–9405.
[5] G. Jian, L. Liu, M.R. Zachariah, Adv. Funct. Mater. 23 (2013) 1341–1346.
[6] C. Rossi, A. Estéve, P. Vashishta, J. Phys. Chem. Solids 71 (2010) 57–58.
[7] E.L. Dreizin, Prog. Energy Combust. Sci. 35 (2009) 141–167.
[8] A. Ali, S. Son, M. Hiskey, D. Naud, J. Propul. Power 20 (2004) 120–126.
[9] C. Rossi, S. Orieux, B. Larangot, T. Do Conto, D. Esteve, Sens. Actuators A 99 (2002) 125–133.
[10] N.H. Yen, L.Y. Wang, Propellants Explos. Pyrotech. 37 (2012) 143–155.
[11] V.E. Sanders, B.W. Asay, T.J. Foley, B.C. Tappan, A.N. Pacheco, S.F. Son, J. Propul. Power 23 (2007) 707–714.
[12] M.A. Ilyushin, I.V. Tselinsky, I.V. Shugalei, Cent. Eur. J. Energetic Mater. 9 (2012) 293–327.
[13] M.R. Weismiller, J.Y. Malchi, R.A. Yetter, T.J. Foley, Proc. Combust. Inst. 32 (2009) 1895–1903.
[14] S. Yan, G. Jian, M.R. Zachariah, ACS Appl. Mater. Interfaces 4 (2012) 6432–6435.
[15] M.R. Weismiller, J.Y. Malchi, J.G. Lee, R.A. Yetter, T.J. Foley, Proc. Combust. Inst. 33 (2011) 1989–1996.
[16] K. Moore, M.L. Pantoya, S.F. Son, J. Propul. Power 23 (2007) 181–185.
[17] M.L. Pantoya, J.J. Granier, Propellants Explos. Pyrotech. 30 (2005) 53–62.
[18] G. Jian, J. Feng, R.J. Jacob, G.C. Egan, M.R. Zachariah, Angew. Chem. Int. Ed. 52 (2013) 9743–9746.
[19] J.J. Granier, M.L. Pantoya, Combust. Flame 138 (2004) 373–383.
[20] K.J. Blobaum, M.E. Reiss, J.M. Plitzko, T.P. Weihs, J. Appl. Phys. 94 (2003) 2923–2929.
[21] M. Petrantoni, C. Rossi, L. Salvagnac, V. Conédéra, A. Estève, C. Tenailleau, P. Alphonse, Y.J. Chabal, J. Appl. Phys. 108 (2010) 084323.
[22] K. Zhang, C. Rossi, G.A. Ardila Rodriguez, Appl. Phys. Lett. 91 (2007) 113117.
[23] S.M. Umbrajkar, S. Seshadri, M. Schoenitz, V.K. Hoffmann, E.L. Dreizin, J. Propul. Power 24 (2008) 192–198.
[24] T.S. Ward, W. Chen, M. Schoenitz, R.N. Dave, E.L. Dreizin, Acta Mater. 53 (2005) 2909–2918.
[25] S.H. Kim, M.R. Zachariah, Adv. Mater. 16 (2004) 1821–1825.
[26] T.M. Tillotson, A.E. Gash, R.L. Simpson, L.W. Hrubesh, J.H. Satcher Jr., J.F. Poco, J. Non-Cryst. Solids 285 (2001) 338–345.
[27] H. S. Seo, J. K. Kim, J. W. Kim, H. S. Kim, K. K. Koo, J Ind. Eng. Chem. 2013 (in press). doi: 10.1016/j.jiec.2013.04.008.
[28] C. Rossi, K. Zhang, D. Esteve, P. Alphonse, P. Tailhades, C. Vahlas, J. Microelectromech. Syst. 16 (2007) 919–931.
[29] S. Subramanium, S. Hasan, S. Bhattacharya, Y. Gao, S. Apperson, M. Hossain, R.V. Shede, S. Gangopadhyay, R. Render, P. Kapper, S. Nicolich, Mater. Res. Soc. Symp. Proc. 896 (2005) 9–14.
[30] R. Shende, S. Subramanian, S. Hasan, S. Apperson, R. Thiruvengadathan, K. Gangopadhyay, S. Gangopadhyay, P. Redner, D. Kapoor, S. Nicolich, W. Balas, Propellants Explos. Pyrotech. 33 (2008) 122–130.
[31] J.Y. Malchi, T.J. Foley, R.A. Yetter, ACS Appl. Mater. Interfaces 1 (2009) 2420–2423.
[32] F. Séverac, P. Alphonse, A. Estève, A. Bancaud, C. Rossi, Adv. Funct. Mater. 22 (2012) 323–329.
[33] H.Y. Wang, G.Q. Jian, S. Yan, J.B. DeLisio, C. Huang, M.R. Zachairiah, ACS Appl. Mater. Interfaces 5 (2013) 6797–6801.
[34] I.G. Loscertales, A. Barrero, I. Guerrero, R. Cortijo, M. Marquez, A.M. Ganan-Calvo, Science 295 (2002) 1695–1698.
[35] N. Bock, T.R. Dargaville, M.A. Woodruff, Prog. Polym. Sci. 37 (2012) 1510–1551.
[36] G. Jian, S. Chowdhury, K. Sullivan, M.R. Zachariah, Combust. Flame 160 (2013) 432–437.
[37] K. Sullivan, M.R. Zachariah, J. Propul. Power 26 (2010) 467–472.
[38] G. Jian, N.W. Piekiel, M.R. Zachariah, J. Phys. Chem. C 116 (2012) 26881–26887.
[39] A. Jaworek, A.T. Sobczyk, J. Electrostatics 66 (2008) 197–219.
[40] K.T. Sullivan, N.W. Piekiel, C. Wu, S. Chowhury, S.T. Kelly, T.C. Hufnagel, K. Fezzaa, M.R. Zachariah, Combust. Flame 159 (2012) 2–15.
[41] P. Chakraborty, M.R. Zachariah, Combust. Flame (2013), http://dx.doi.org/10.1016/j.combustflame.2013.10.017.